

Design, Fabrication and Control of A Six-Legged Robot For Search and Rescue

**Noel David¹, V.G. Umasekar², G.S.Bala Maga Ganapathi³,
Shreyaank Raje Urs R⁴**

¹ *PG Student, Robotics, Department of Mechanical engineering, SRM University, Chennai*

² *Assistant Professor (O.G), Department of Mechanical Engineering, SRM University, Chennai*

³ *PG Student, Robotics, Department of Mechanical engineering, SRM University, Chennai*

⁴ *PG Student, Robotics, Department of Mechanical engineering, SRM University, Chennai*

Abstract

The objective of the project is to design, fabricate and control the locomotion of a six-legged robot for the purpose of rescue aiding. The ability of the robot to produce multiple gait sequences makes travelling across irregular terrain patterns possible. The important feature of the developing model is that the robot has good control actuations. Good control actuations enable the robot to move efficiently through various obstacles. This robot can climb into ruins to detect the presence of casualties by using P-IR sensor and live video streaming.

Keywords: Six-legged, Gait, P-IR sensor, Irregular Terrain

Introduction

With the world's population increasing and more people living in urban environments, both man-made and natural catastrophes are becoming more and more common. Those has been illustrated in recent events such as the terrorist attacks on the World trade Center in 2001, and hurricane Katrina in the USA. During disasters in urban areas, it is common for buildings to collapse and for debris to be present, complicating the search and rescue process. Such environments make survivors difficult to find amongst the debris, because they may be buried. Additionally, debris and partially-collapsed buildings can also make the search environment dangerous. In an event where lives are at risk, time is always critical. Rescue workers need up-to-the-minute information about the hazards they face and where the survivors may lie.

In nature, the cockroach is one of the creatures that exhibit excellent mobility in various types of terrain. It is able to climb rock field, mud, sand, vegetation, railroad tracks, and up slopes. This property of mobility is attempted to be recreated in robots that look and move like cockroaches. Cockroach type robots usually have six compliant legs, each possessing one independently actuated revolute degree of freedom (DOF).

This work aims at developing a cockroach type robot and outlines expectations for future development. These robots may play a crucial role in search and rescue operations. The highly articulated body allows the robot to traverse difficult terrains such as collapsed buildings.

This robot could make its way through destroyed buildings looking for people, while simultaneously bringing communication equipment together with small amount of food and water to anyone trapped in the shattered building. A P-IR sensor is used for detecting the presence of human and a visual camera is used as its aid. GPS transmitter and Wi-Fi network system is incorporated for communication with the ground base to inform about casualties in the War field.

Design of The Robot

3D modeling software was used to design the model of the Six-Legged Robot. The model will be with a rigid aluminum structure as the robot body with a fiber glass cover at the top and 6 legs made of spring steel and coated with a rubber like material on the outer surface. Each model of the segment were created separately and assembled.

A. Body of The Robot

Body is made of Strain Hardened And Partially Annealed Aluminum of grade-H2. Its thickness is 1.5mm and its density of $Al=2.7 \text{ g/Cm}^3$. 600*300 rectangular shaped body is made out of it as shown in the Fig. 1, and Fig.2. The middle leg distance from each other is increased so that the length of the robot is reduced and also the limitation posed to the leg movement is terminated. The construction of the robot body as per its dimensions is made in the SOLIDWORKS Software and the material type is selected to come up with the computer generated results of the weight of the body.

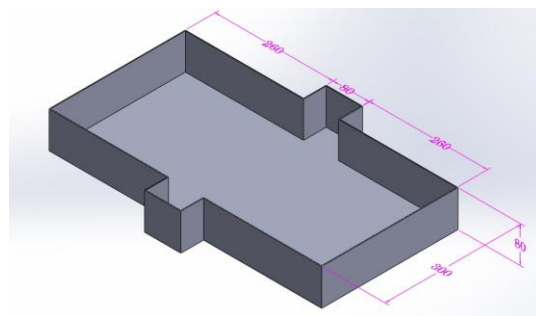


Figure 1: Solid works Generated Model of The Body



Figure 2: Fabricated Body of The Robot

B. Leg of The Robot

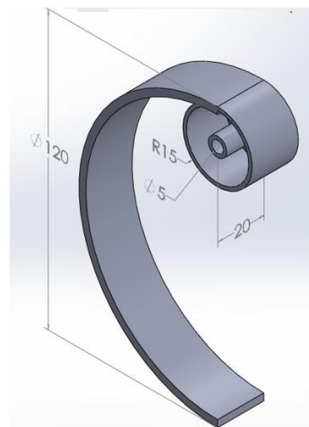


Figure 3: Solid works Generated Model of The Leg



Figure 4: Fabricated Leg of The Robot

Leg is made of 301 Spring tempered stainless steel of Grade-A666. Density Of Spring Steel= $7.8\text{g}/\text{Cm}^3$ and the thickness of the wheel is 3mm. Spring Steel is selected as the leg material as it can withstand any kind of tension and load acting upon it without permanent deformation. The height of the leg is 120mm as shown in

Fig. 3 and Fig. 4. On the outer side of the leg is a layer of rubber with a zig-zag profile to provide better contact with the ground.

Robot Parameters[4]

Robot uses pairs of contra lateral legs in phase on level ground, it is very effectively anchored to the sagittal plane, and so here we develop a planar model for robot ($d:=2$), with only two legs modeled, each with one joint ($n:= 2, q= 5$) [4]

The body is allowed to contact the ground at up to two locations (front and rear), so that $k \leq 4$.

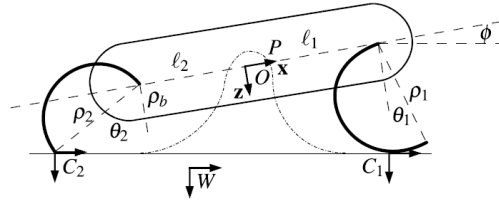


Figure 5: Coordinate Frames and Key Dimensions For Robot Under The Self-Manipulation Formulation

Table 1: Symbol and Definitions of the terms used in the explanations

Symbol	Definition
m_b	Body Mass
I_b	Body Inertia
m_l	Leg Mass
I_l	Leg Inertia
l_1, l_2	Body-Hip Length
ρ_1, ρ_2	Leg Length
ρ_b	Body Radius
τ_s	Saturated Maximum Torque

There are thus 2 contact wrenches at each toe and 1 at the front and rear of the robot, implying that $c \leq 6$. [4]

The location and orientation of the various frames are shown in Fig. 5. In the palm frame, let the $+x$ axis be aligned with the robot, $+z$ in the "downward" direction from the robot, and thus $+y$ exiting the page (this is a standard "North, East, Down" orientation). Hip i (S_i) is located l_i away from the P frame along the positive x direction, and the leg length is ρ_i putting the F_i frame at ρ_i along the positive z direction from M_i , thus,

$$g_{pc1}(\theta, \varphi) := [l_1 - \rho_1 \sin\theta_1, \rho_1 \cos\theta_1, -\varphi]^T \quad (1)$$

$$g_{pc2}(\theta, \varphi) := [l_2 - \rho_2 \sin\theta_2, \rho_2 \cos\theta_2, -\varphi]^T \quad (2)$$

When the leg is supported on its toe ($0 \leq \theta_i - \varphi < \pi$), while the leg is in rolling contact

$$g_{pc1}(\theta, \varphi) := [l_1 - \rho_1/2 (\sin\theta_1 + \sin\varphi), \rho_1/2 (\cos\theta_1 + \cos\varphi), -\varphi]^T \quad (3)$$

$$g_{pc2}(\theta, \varphi) := [l_2 - \rho_2/2 (\sin\theta_2 + \sin\varphi), \rho_2/2 (\cos\theta_2 + \cos\varphi), -\varphi]^T \quad (4)$$

The body has semi-circular ends with radius ρ_b about the hips and so the two potential body contact points are,

$$g_{pc3}(\theta, \varphi) := [l_1 - \rho_b \sin\varphi, \rho_b \cos\varphi, -\varphi]^T \quad (5)$$

$$g_{pc4}(\theta, \varphi) := [-l_2 - \rho_b \sin\varphi, \rho_b \cos\varphi, -\varphi]^T \quad (6)$$

The body pitch is $\varphi = 0$ when the robot is horizontal and a positive pitch when hip 1 is higher than hip 2. The leg angles are measured as θ_1 and θ_2 in the clockwise direction from the body +z direction. [4]

Torque Calculation For Motor Selection

Length of the shaft=0.3 m

Load to be moved

weight of the body=1.06 kg

weight of the motor=0.3 kg*6=1.8 kg

weight of the leg=0.06 kg*6=0.36 kg

Total load=3.22 kg== 31.57 N



Figure 6: Squared Geared Motor

Force Required=Load*Acceleration due to gravity

$$=31.57N*9.81$$

$$=309.701 \text{ N}$$

Torque required=Force*Perpendicular Dist

$$=309.701*0.3$$

$$=92.91051 \text{ Nm}$$

$$=9.47 \text{ Kg-cm}$$

The motor in Fig.6, is selected as it matches the torque requirement of the robot and its a 30 RPM, 12V DC motor with squared gear box.



Figure 7: Model of The Robot Built

Components of The Robot

C. ARM7 Processor

ARM7 is a group of older 32-bit ARM processor cores licensed by ARM Holdings. ARM7 processor has instruction set providing improved code density compared to previous designs. This processor is used here for controlling the various activities of the robot combining signals from other components in the robot.

D. Relay Switches

Relay Switch Circuit and relay switching circuits used to control a variety of loads in circuit switching applications. Here this circuit is used to turn on and off different motors for direction control.

E. Proximity Sensors

A proximity sensor is a sensor able to detect the presence of nearby objects without any physical contact. Here the proximity sensors are fixed near the end of each legs. So, when the legs cross the proximity sensor the counter counts to 1 and so on thus enabling better gaits without any tumble in the robot movements.

F. Zigbee Transceiver

ZigBee is a specification for a suite of high-level communication protocols used to create personal area networks built from small, low-power digital radios. Here this ZigBee transceiver acts as wireless transmitter and receiver between the ground level controller and the robot for controlling the robot within a certain area limited to the transceiver's frequency.

G. Ultrasonic Transducer

Ultrasonic transducers are transducers that convert ultrasound waves to electrical signals or vice versa. Those that both transmit and receive may also be called ultrasound transceivers. Here this is used for the purpose of detecting obstacles in its path when it is on a search mission. The signal from the transducer is processed and the robot is navigated accordingly avoiding every obstacle in its path

H. PIR Sensor

A passive infrared sensor (PIR sensor) is an electronic sensor that measures infrared (IR) light radiating from objects in its field of view. They are most often used in PIR-based motion detectors. When the sensor is idle, both slots detect the same amount of IR, the ambient amount radiated from the room or walls or outdoors. When a warm body like a human or animal passes by, it first intercepts one half of the PIR sensor, which causes a positive differential change between the two halves. When the warm body leaves the sensing area, the reverse happens, whereby the sensor generates a negative differential change. This is used for detecting the presence of casualties in the area of search.

I. Video Camera

A video camera along with AV receiver is attached to the robot which enables transmission of LIVE images from the site of search and it helps in two ways either controlling the robot wirelessly or in finding casualties.

J. Battery

A sealed Lead-acid battery is used for the purpose of powering the various components of the robot. The battery's rating is 12V, 7.5Ah which matches with all the components that consume power in the robot.



Figure 8: Various Components of The Robot

Stress Distribution In The Robot

K. Robot Body

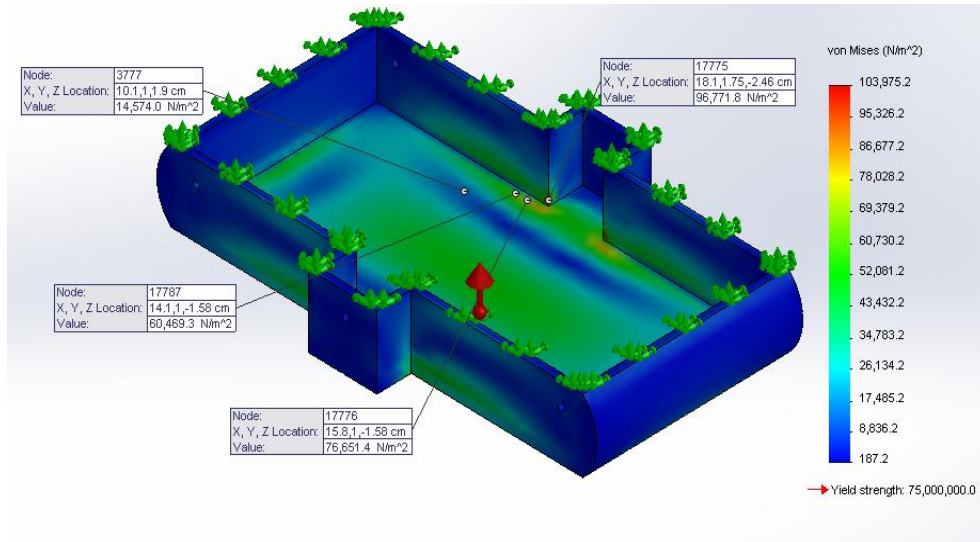


Figure 9: Stress Distribution on Robot Body

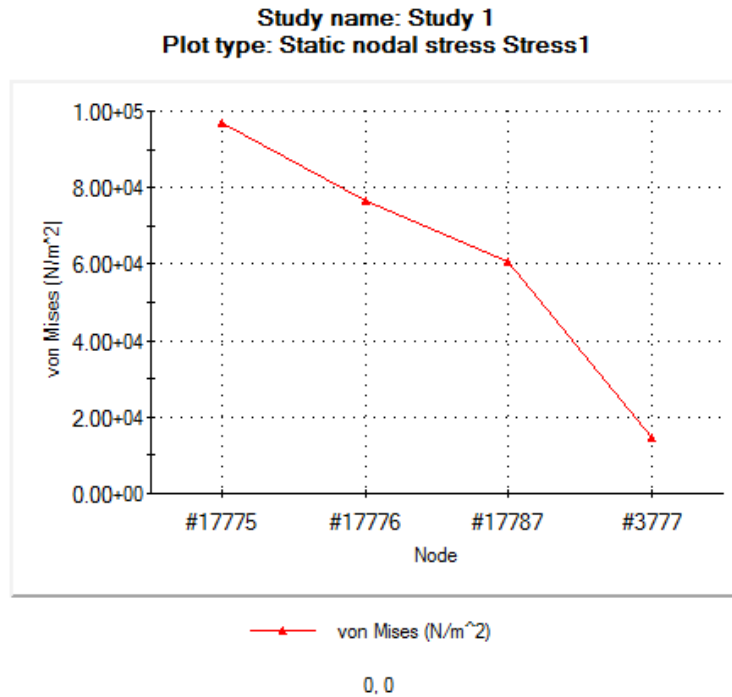


Figure 10: Stress Distribution Graph Indication Maximum and Minimum Stress

It is seen from the stress distribution diagram in Fig.9 that the corners of the robot body experience more stress when compared to the free ends.

L. Robot Leg

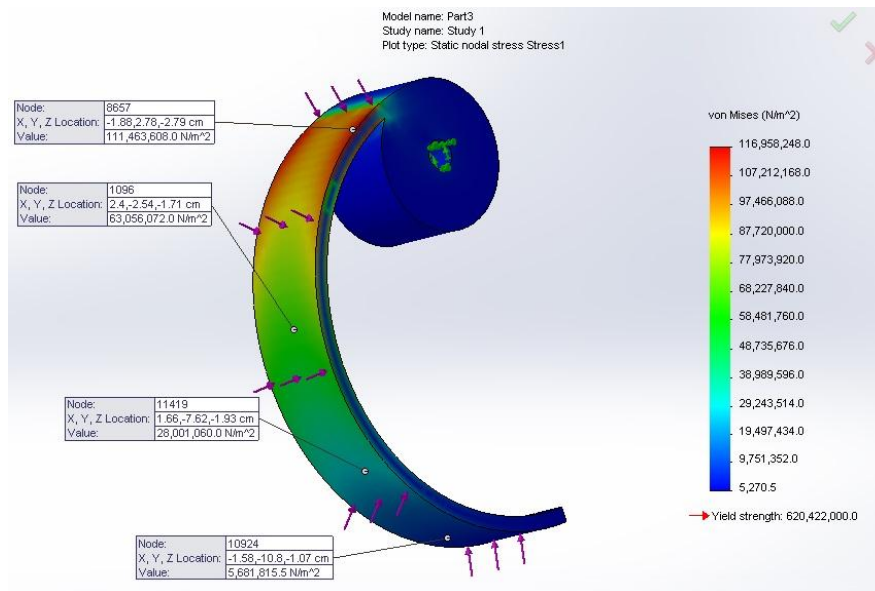


Figure 11: Stress Distribution on Robot Leg

From the graph in the Fig.10, the maximum and minimum stress at different location on the body of the robot is plotted to show the range of stress involved.

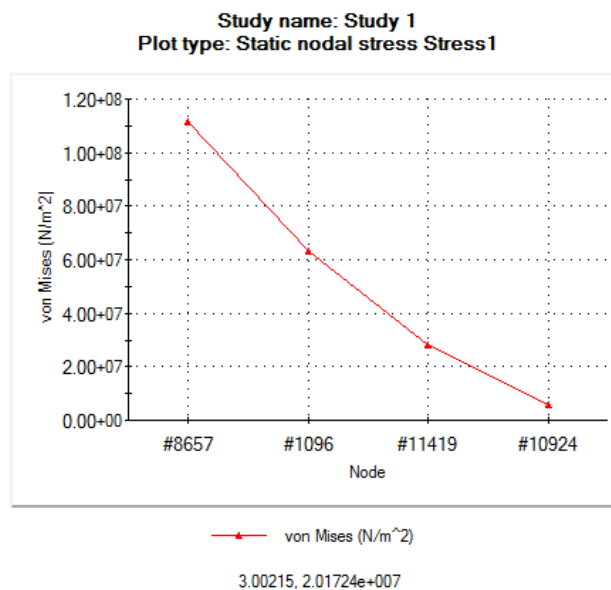


Figure 12: Stress Distribution Graph Indication Maximum and Minimum Stress

The Fig.11, shows that the connecting area between the shaft and the leg experience more stress but it is within a certain range that it does not permanently deform the legs which makes this a perfect design.

From the graph in the Fig.12, the maximum and minimum stress at different location on the body of the robot is plotted to show the range of stress involved.

Mechanism of The Robot Run

The integral activities of the robot are controlled by the ARM7 processor.

The six motors are connected to the motor driver circuit and also to the relay switches.

The relay switches change the direction of rotation of the motors as per the control signals it receives from the controller.

The ZigBee transceiver is connected to the robot as well as the remote controller, which is a laptop in this case.

A video camera is attached to the robot to get LIVE images of the environment where the robot is located to enable controlling from a remote location.

The ARM7 processor can be coded using C language and the program to make the robot move forward backward, right, and left is written and fed into the processor. Thus through the radio control the navigation of the robot is achieved.

In order to make the robot autonomous, the robot is connected to ultrasonic sensor to detect the obstacles and alter its path on its own. The robot cannot be made completely autonomous as it is hard for the robot to locate itself and map the area from the ground view.

The most important feature of this robot is the presence of proximity sensors at the path of rotation of each leg. If the leg crosses the sensor visibility the counter counts to 1 and so on. This helps in keeping account of what is the approximate location of the leg for better gait sequences.

In general two motor drivers are used to control the six motors (3 motors for each driver). The alternate motors are connected to the motor drivers as described in the Fig. 13, differentiated by (1) and (2).

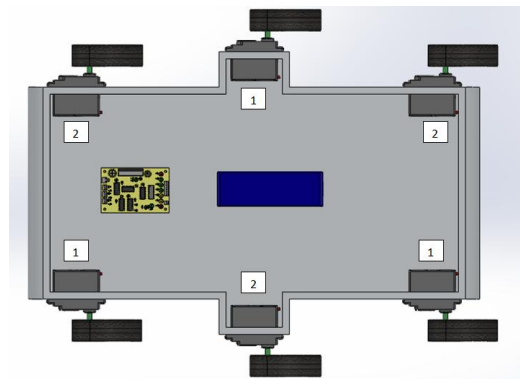


Figure 13: Motor Driver Connections

P-IR sensor is used in the robot to indicate the presence of casualties in areas where it is carrying out the search operation.

Sometimes color detection from the video camera images is done using programming for identifying casualties from the war field based on the uniform color.

This makes the robot very efficient equipment for the search and rescue operation.

Calculations

M. Rolling Resistance

$$\begin{aligned} & * \text{Rolling Resistance} = (\text{Resistance Coefficient} * \\ & \quad \text{Mass} * \text{Acceleration}) / \\ & \quad \text{Radius of the wheel} \\ & = (0.5 * 3.22 * 9.81) / 120 \\ & = 0.131 \text{ N (with dimension length)} \end{aligned}$$

$$\begin{aligned} & * \text{Rolling Resistance} = (\text{Resistance Coefficient} * \\ & \quad \text{Mass} * \text{Acceleration}) \\ & = (0.004 * 3.22 * 9.81) \\ & = 0.126 \text{ N (dimensionless)} \end{aligned}$$

By computing the resistance of the wheel using the two methods either by using dimension length components or dimensionless components we get the rolling resistance value almost in the same range.

Table 2: Forward Velocity of The Robot on Various Terrains

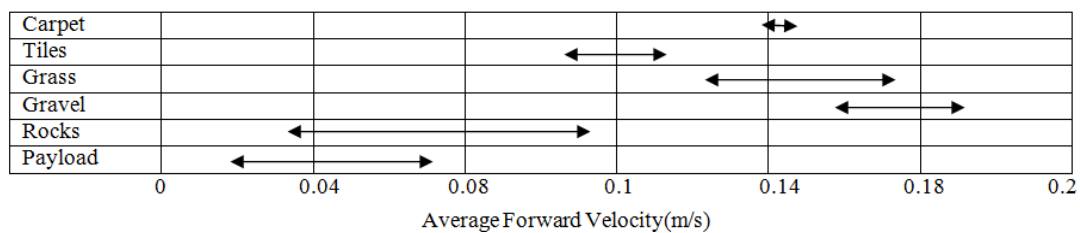


Table 3: Comparison between other Hexapods and this robot

Name	L (m)	M (kg)	V (m/s)	V/L
Case Western Robot II	0.5	1	0.083	0.16
Dante II	3	770	0.017	0.006
Atilla	0.36	2.5	0.03	0.083
Genghis	0.39	1.8	0.038	0.097
Adaptive Suspension Vehicle	5	3200	1.1	0.22
Boadicea	0.5	4.9	0.11	0.22
Six Legged Rescue Robot	0.44	3.7	0.18	0.409

L = body length, M = robot mass, V = maximum speed.

N. Velocity

$$\begin{aligned} \text{Velocity} &= (\pi * \text{Diameter of Wheel} * \\ &\text{Rotation per min of robot}) / 60 \\ &= (3.14 * 120 * 10^{-3} * 30) / 60 \\ &= 0.188 \text{ m/s (no load condition)} \end{aligned}$$

The computation of the velocity shows the maximum velocity of the robot and it can vary according to the terrain it is moving on as shown in the Table.2 which is tabulated by running the robot on the corresponding terrain.

The Table.3, shows the comparison between the various Hexapods and this robot comparing their dimension, mass and velocity.

Conclusion

In this work, a six-legged robot with novel structures and highly integrated sensor systems is developed. A complete sensor system is designed to make the robot have the perception of environment and its own state. The proximity sensor employed near the legs help in finding the angle at which the legs are located. This helps in producing better contact between the legs and ground generating better gait sequences to move on irregular terrains and carrying out its task of search and rescue.

Future Work

Stress sensors can be used on the robot legs to identify the stress on the legs on different terrain. By keeping account of the stress developed on different terrains the speed of the motor is alternatively altered so that the destination can be reached with more faster without causing any damage to the robot body due to rough terrain conditions. Thus by using stress sensors on the robot leg the safety of the robot is ensured along with better speed gaits.

References

- [1] Yasemin Ozkan Aydin , Afsar Saranli , Yigit Yazicioglu , Uluc Saranli , Kemal Leblebicioglu “Optimal control of a half-circular compliant legged monopod” Transactions of Control Engineering Practice pp.10–21, 5 August 2014.
- [2] He Zhang, Yubin Liu, Jie Zhao, Jie Chen and Jihong Yan “Development of a Bionic Hexapod Robot for Walking on Unstructured Terrain” Journal of Bionic Engineering pp.176–187, 2014.
- [3] Mine Cuneyitoglu Ozkul, Afsar Saranli and Yigit Yazicioglu “Acoustic surface perception from naturally occurring step sounds of a dexterous hexapod robot” Transactions of Mechanical Systems and Signal Processing pp.178–193, 25 May 2013.
- [4] Aaron M. Johnson and Daniel E. Koditschek “Legged Self-Manipulation”, in IEEE International Journal on Robotics and Automation, May 16, 2013.

- [5] Samuel N. Cubero “Design concepts for a hybrid swimming and walking vehicle” International Symposium on Robotics and Intelligent Sensors pp. 1211 – 1220, 2012.
- [6] Fei Li, Weiting Liu, Xin Fu, Gabriella Bonsignori, Umberto Scarfogliero, Cesare Stefanini, Paolo Dario “Jumping like an insect: Design and dynamic optimization of a jumping mini robot based on bio-mimetic inspiration” Transactions of Mechatronics pp.167–176, 30 January 2012.
- [7] García-Lopez, M.C, Gorrostieta-Hurtado, E, Vargas-Soto, E., Ramos-Arreguín, J.M, Sotomayor-Olmedo, A and Moya Morales J.C. “Kinematic analysis for trajectory generation in one leg of a hexapod robot” 2012 Iberoamerican Conference on Electronics Engineering and Computer Science.
- [8] Servet Soyguder , Hasan Alli “Kinematic and dynamic analysis of a hexapod walking–running–bounding gaits robot and control actions” Transactions of Computers and Electrical Engineering pp.444–458, 10 November 2011.
- [9] Shu-Hung Liu, Tse-Shih Huang, Jia-Yush Yen “Comparison of sensor fusion methods for an SMA-based hexapod biomimetic robot” Transactions of Robotics and Autonomous Systems pp. 737-744, 27 November 2009.
- [10] Christina Georgiades, Meyer Nahon , MartinBuehler “Simulation of an underwater hexapod robot” Transactions of Ocean Engineering pp.39–47, 24 November 2008.
- [11] Richard J. Bachmann , Frank J. Boria , Ravi Vaidyanathan , Peter G. Ifju and Roger D. Quinn “A biologically inspired micro-vehicle capable of aerial and terrestrial locomotion” Transactions of Mechanism and Machine Theory pp.513–526, 8 October 2008.

18750

Noel David